arXiv:0704.2548v2 [physics.ins-det] 2 Jun 2007

# Triggering at High Luminosity Colliders

**Hans Peter Beck**

Laboratory of High Energy Physics, University of Bern, Sidlerstr. 5, 3012 Bern, CH

E-mail: hans.peter.beck@cern.ch

**Abstract.** This article discusses the techniques used to select online promising events at high energy and high luminosity colliders. After a brief introduction, explaining some general aspects of triggering, the more specific implementation options for well established machines like the Tevatron and Large Hadron Collider are presented. An outlook on what difficulties need to be met is given when designing trigger systems at the Super Large Hadron Collider, or at the International Linear Collider.

## 1. Introduction

Exploring nature at higher and higher energies of particle collisions has been proven to be a successful road to deepen our understanding of the structure of matter. It has let to the formulation of the standard model, which explains nature at its smallest scales and biggest energy densities reachable by todays largest machines. On the other hand, the standard model is almost certainly not the final word of a theory describing nature at all scales and new phenomena, not contained within the framework of the standard model, necessarily exist. Such new phenomena are often referred to as *new physics*.

Colliding particles at the highest possible energies has the potential to unveil manifestations of new physics, but these will necessarily be covered within a huge background of already well known standard model processes. Not only need the energy scale of the particle collisions be pushed to the highest possible values, but also the collision rate, i.e. the machine luminosity, needs to be pushed to unprecedented values. In consequence, new or interesting physics events will be covered by a large amount of well established standard model processes.

Todays largest collider complexes are the actual running Tevatron at the Fermi National Accelerator Laboratory, Batavia, IL in the United States and the soon to be completed LHC at CERN, Geneva, Switzerland.

Tevatron, which since its upgrade is referred to as Tevatron Run II brings protons to collision with anti-protons at a centre of mass energy of $\sqrt{s} = 1.96$ TeV at a peak luminosity of $\mathcal{L} = 2{-}3 \times 10^{32}\,\mathrm{cm}^{-2}\mathrm{s}^{-1}$. The interval between subsequent beam-crossings amounts to 396 ns, corresponding to a beam-crossing rate of 2.5 MHz.

Two general-purpose experiments, DØ [1] and CDF [2] are recording those proton–anti-proton collisions passing their respective trigger schemes.

The Large Hadron Collider (LHC) is a proton-proton super-conducting collider operating at $\sqrt{s} = 14$ TeV at a nominal luminosity of $\mathcal{L} = 10^{34}\,\mathrm{cm}^{-2}\mathrm{s}^{-1}$. The beam-crossing period for proton-proton collisions at the LHC is 25 ns, corresponding to a crossing rate of 40 MHz. At design-luminosity, $O(10^9)$ inelastic proton-proton collisions will occur, implying an average of about 25 interactions per bunch crossing.

Two general-purpose experiments, ATLAS [3] and CMS [4] and three purpose built experiments, ALICE [5], LHCb [6] and TOTEM [7] are in their final stages of installation and commissioning. LHCb is a dedicated B-physics experiment with the aim of measuring the subtle differences between matter and anti-matter. TOTEM is a dedicated experiment to measure the total cross-section, elastic scattering and diffractive processes of proton-proton collisions at the LHC. ALICE will study the physical properties of matter during the early stages after the big bang, for which LHC will also provide heavy-ion lead-lead collisions.

### *1.1. Physics goals, cross-sections and event rates*

At high luminosity hadron colliders discovery physics is the main issue, which requires sensitivity of the trigger to a wide range of signatures predicted by various theoretical

models within and beyond the Standard Model.

Cross-sections and event rates for proton proton collisions at the Tevatron and LHC colliders are shown in figure 1 as a function of the produced particle mass or the highest jet transverse energy. New physics, such as the yet to be discovered Higgs particle or manifestations of super-symmetric particles happens in just one out of $\mathcal{O}(10^8 \cdots 10^{13})$ or even fewer proton-proton collisions.

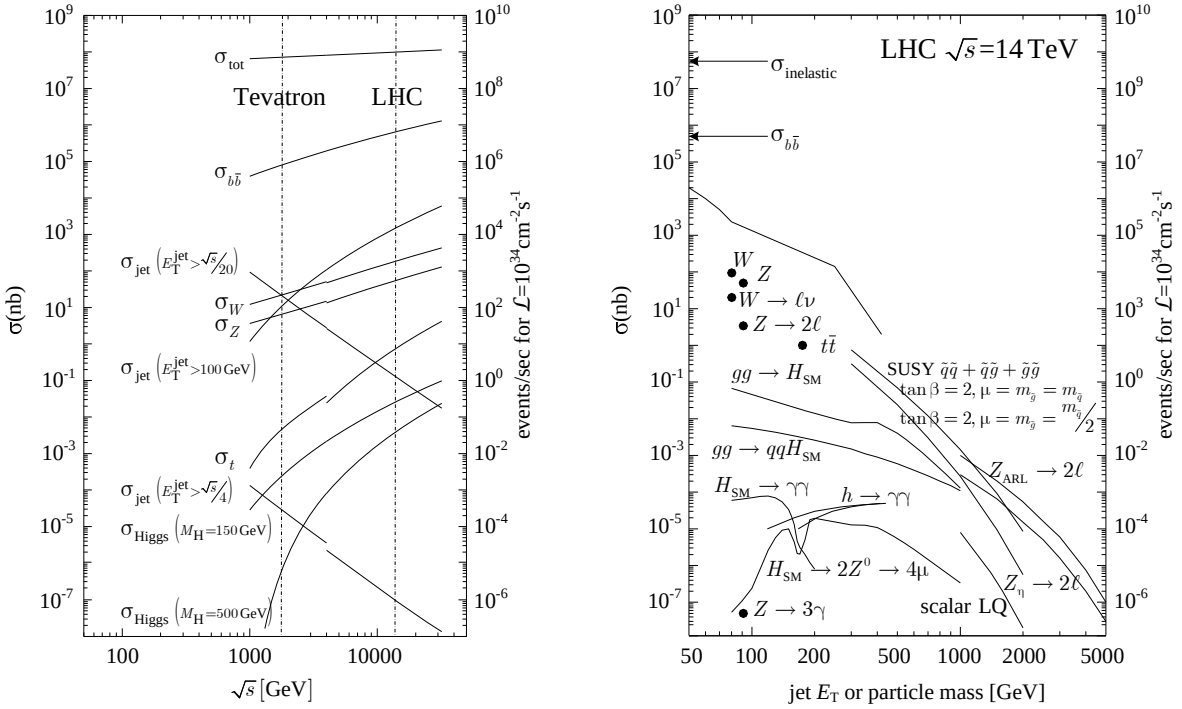


**Figure 1.** Cross-sections and event rates for proton proton collisions
left) as a function of the centre of mass energy covering Tevatron ($p - \bar{p}$ collision) and LHC ($p - p$ collision) energy scales (figure reproduced from [8]).
right) as a function of the produced particle mass or the highest jet transverse energy for $\sqrt{s} = 14$ TeV (figure reproduced from [9]).

Reading out the detector data at the fixed beam crossing rate and analyzing the data off-line is beyond imagination of todays data acquisition, data storage, and data processing systems. A powerful selection mechanism is therefore needed to select, as early as possible in the data acquisition chain, only those particle collisions promising to contain interesting physics while simultaneously reducing the overall data rate by many orders of magnitude.

This is the role of the trigger, which e.g. at the Tevatron detectors CDF and DØ reduce the initial beam crossing rate by $\mathcal{O}(10^4)$, and at the LHC detectors ATLAS and CMS by $\mathcal{O}(10^5)$. One has to note here that the number of proton-proton collisions is, due to multiple interactions per beam crossing, in average $3 - 4$ times larger than the beam crossing rate at the Tevatron collider and even $\sim 25$ times larger at the LHC. Given that only one of these multiple interactions give raise to a trigger signal, one can also

state that the actual physics selection of the trigger system selects one proton-proton collision out of $\mathcal{O}(10^5)$ at CDF and DØ and one out of $\mathcal{O}(10^7)$ at ATLAS and CMS. The data acquisition system, however, can not distinguish between the actual proton-proton collision that activated the trigger and the extra collisions that took place within the same beam crossing. All proton-proton collisions in a beam crossing are read-out simultaneously; in analogy of looking at a photo that has been exposed multiple times. This changes terminology of what is meant by an event. Often, an event is referred to as all the tracks and energy deposits for a single proton-proton collision. However, in high luminosity colliders, a event is whatever tracks and energy deposits are read out per beam crossing. Tracks and energy deposits, not originating from the primary proton-proton collision that caused the trigger to fire, is called *pile-up*.

Precision measurements in contrast to discovery physics are often severely disturbed in the presence of large pile-up. Therefore, data taken when instantaneous luminosity is reduced; e.g. in the start-up phase of a new accelerator (assuming an already well understood detector) or at the end of an accelerator coasts, has much reduced pile-up and thus provides a cleaner environment to allow for some precision studies – at the cost of a reduced statistical data set for the analysis.

## 2. Trigger strategies

A powerful and flexible trigger is the cornerstone of a modern high energy and high luminosity collider experiment. It dictates what physics processes can be studied properly and what is ultimately left unexplored. The trigger must also offer sufficient flexibility to respond to changing physics goals and to new ideas. If the trigger is not able to achieve sufficient selectivity to meet these requirements, the physics potential of the experiment will be seriously compromised.

In an idealistic high energy physics experiment, enough bandwidth and enough CPU power would be available to analyze every single proton-proton collision and then decide whether the event contained interesting physics. In real life, available resources are limited and trigger strategies based on the existence of one or few trigger objects need to be implemented in a cost efficient manner.

### *2.1. Trigger objects*

Features that distinguish interesting and/or new physics from the bulk of Standard Model processes at colliders are typically the presence of high-$p_{\mathrm{T}}$ leptons ($e, \mu, \tau$), photons, and jets, or large missing transverse energy (neutrinos, or other weakly or non interacting new particles), as they occur in very hard interactions or as decay products from new heavy particles. Especially clean signatures arise if the leptons, photons or non-interacting particles are not covered inside jets but are *isolated*.

*2.1.1.* **High-$p_{\mathrm{T}}$ leptons** Triggering on high-$p_{\mathrm{T}}$ leptons provides the primary means of selecting events containing W, Z and Higgs bosons in $W \to l\nu$, $Z \to l\bar{l}$, $H \to Z^{(*)}Z \to 4l$ decays, as well as super-symmetric particles in $\chi_2^0 \to l\tilde{l}$, $\tilde{l} \to \chi_1^0 l$ decays. Leptons can also tag heavy quarks such as $t \to bW$ and $b$'s through their semi-leptonic decays. In the latter, a $b$-tag can be obtained through a lifetime selection of the relatively long lived B-meson, which leads to non-pointing high-$p_{\mathrm{T}}$ leptons with respect to the primary interaction vertex.

Triggering on high-$p_{\mathrm{T}}$ tau-leptons can lead to increase in statistical samples, where the high-$p_{\mathrm{T}}$ electron- and muon-trigger samples need to be enhanced. However, the signature of tau's is all but clean due to leptonic decays of the tau into a lighter lepton and two neutrinos $\tau \to l\nu_l\nu_\tau$ or its semi-leptonic decays into hadrons and a tau neutrino $\tau \to h\nu_\tau$.

In the pure leptonic case, the electron- or muon-trigger have a chance to select tau events in cases where the energy carried away by the escaping neutrinos is not too high and the transverse momentum $p_{\mathrm{T}}$ of the decay lepton is still above the trigger threshold.

Semi-leptonic tau-decays can be triggered by means of isolated, high-$p_{\mathrm{T}}$ tracks or very narrow jets.

High-$p_{\mathrm{T}}$ tau-triggers are more complex than other lepton triggers, still they provide an important handle to new physics. For instance, due to the relative strong coupling of tau to the Higgs particle, which is enhanced with respect to the coupling to lighter leptons as $m_\tau^2/m_l^2$, the decay mode $H \to \tau\tau$ is of interest for Higgs discovery in the low Higgs mass region [10]. In some of the large $\tan\beta$ SUSY scenarios, $H \to \tau\tau$ is grossly enhanced over a wide range of Higgs mass [11].

*2.1.2.* **High-$p_{\mathrm{T}}$ photons** Triggering on high-$p_{\mathrm{T}}$ photons is of prime interest for light Higgs searches, such as $H \to \gamma\gamma$, as a very clean signal is expected for Higgs masses below ∼120 GeV [12, 13].

On the other hand, high-$p_{\mathrm{T}}$ photons occurring in QCD processes via quark-gluon Compton scattering or quark-anti-quark annihilation are often seen as background for the quest of new physics. Nevertheless, these photons are useful in global fits providing parton density functions to be used in Monte Carlo simulations [14].

Photons from highly energetic $\pi^0$ and $\eta$ mesons are a major background to prompt photon signals. As these mesons are produced within jets, an isolation criteria can be used to suppress such photons. Photons originating from High-$p_{\mathrm{T}}$ electrons undergoing Bremsstrahlung are another source of background, which can be suppressed after reconstruction of the electron track, and after identification of a kink in the electron track.

*2.1.3.* **High-$p_{\mathrm{T}}$ jets** Triggering on high-$p_{\mathrm{T}}$ jets is hampered by the fact that jets are produced abundantly in hadron colliders, as the standard QCD processes $q+q \to q+q$, $q+g \to q+g$, $g+g \to g+g$ with one or more extra gluons produced by QCD Bremsstrahlung.

High-$p_{\mathrm{T}}$ jets which can hint for new physics occur from $p + p \rightarrow X \rightarrow q + (q, l, ...)$, with X being a new heavy particle decaying hadronically into quark-quark, quark-lepton, or quark + missing energy.

As the cross section for high-$p_{\mathrm{T}}$ QCD jets is dropping more steeply than the expected cross section for jets stemming from new heavy particles they can be distinguished statistically in the high energy end range of the jet energy spectrum.

It is therefore useful to look for combinations of multiple high-$p_{\mathrm{T}}$ jets, high-$p_{\mathrm{T}}$ jets plus leptons or high-$p_{\mathrm{T}}$-jets plus missing energy in order to reach conclusive results about possible heavy states in proton-proton collisions.

Another possible way to improve the signal to noise ratio stemming from QCD jets is to select those jets only that manifest from the hadronization of a $b$-quark. With the $b\bar{b}$ production cross section being $\mathcal{O}(10^2)$ lower than the production of light di-quarks, signal to noise ratios can be expected up to $\mathcal{O}(10)$ enhanced, depending on the process under study.

Higgs searches in the low mass region relying solely on a $b$-tag to search for $H \rightarrow bb$ events is close to impossible for reasons of bandwidth and CPU power available for the trigger selection processing, because the $b\bar{b}$ production rate is $\mathcal{O}(MHz)$. In associated Higgs production, where besides the Higgs particle also two top-quarks are produced, as in $p + p \rightarrow t + \bar{t} + H$, the $H \rightarrow bb$ process can be searched for. This requires a multi-object trigger, with asking for two $b$-tagged jets from the $H \rightarrow bb$ decay, another two $b$-tagged jets from the two top-quark decays with $t \rightarrow Wb$ and depending on the decay modes of the W-boson a lepton tag from the $W \rightarrow l\nu$ decay or two light-quark jets from the $W \rightarrow q_u q_d$ and $W \rightarrow q_c q_s$ decays.

*2.1.4.* **Missing energy** Triggering on missing energy is a window for new physics occurring from $p + p \rightarrow X$, with $X$ being one or more new heavy particles which are either stable and non-interacting with the surrounding detector elements, or which decay into particles of which at least one escapes detection due to non-interaction with the surrounding detector elements. Important for missing energy is that the invisible particle carries away a large amount of the available energy in transverse direction to the beam line. Missing energy combined with leptons/photons or jets can be a manifestation of the presence of large extra dimensions, different SUSY configurations, or other new physics beyond the Standard Model.

Events containing multiple leptons and missing energy are often referred to as the *gold-plated* SUSY discovery mode.

Obviously, missing energy can occur also due to detector inefficiencies, dead areas, noise, as well as non-hermeticity of the detector. Still, triggering on missing energy is key for the quest in finding new physics, which requires a detailed understanding of the detector response.

*2.1.5.* **Total scalar sum of transverse energy** Triggering on total scalar sum of all transverse energy deposits in all calorimeter cells and without further requirements on

the event topology allows for an open search for new heavy state particles. However, the summing up of all calorimetric cell energy deposits can be very susceptible to both noise and pile-up effects and cannot be easily calibrated unlike calibrating individual jet energies. Therefore a modified total scalar transverse energy sum $H_{\mathrm{T}}$ is used instead. Experiments usually define $H_{\mathrm{T}}^{\mathrm{calo}}$ as the sum over the leading jet's transverse energies:

$$H_{\mathrm{T}}^{\mathrm{calo}} = \sum_{\mathrm{jets}} E_{\mathrm{T}}^{\mathrm{jet}}$$

Often the leptons transverse energies and $E_{\mathrm{T}}^{\mathrm{miss}}$ are also added:

$$H_{\mathrm{T}} = H_{\mathrm{T}}^{\mathrm{calo}} + \sum_{\mathrm{muons}} E_{\mathrm{T}}^{\mu} + E_{\mathrm{T}}^{\mathrm{miss}}$$

Note that electrons and to some extent taus, via the electron from the $\tau \to e\nu_e\nu_\tau$ decay, are already accounted for in $H_{\mathrm{T}}^{\mathrm{calo}}$.

The $H_{\mathrm{T}}$ trigger can capture high jet multiplicity events such as those from fully hadronic top decay, hadronic decays of squarks and gluinos. These events have a total transverse energy of several hundred GeV. They may actually fail the jet triggers because individual jet transverse energies can be softer than the sustainable thresholds of individual- and multi-jet triggers.

### *2.2. Trigger chains*

In a first step, the trigger has to identify the trigger objects in every event. Identifying e.g. an isolated high-$p_{\mathrm{T}}$ electron and measuring at least its transverse momentum is a multi-step procedure. In an initial step, energy deposits in the trigger towers of the electro-magnetic calorimeter need to be looked for and pattern recognition is needed to identify close-by energy deposits as a single energy cluster and then to determine the total energy deposit, and the centre of the cluster. Furthermore, pattern recognition needs to identify whether the cluster is well isolated from other energy deposits and especially whether it is well isolated from energy deposits in the hadronic calorimeter, which usually follows the electro-magnetic calorimeter. After these steps, an isolated electromagnetic cluster is identified that could either stem from an isolated electron or photon. Distinguishing the two cases requires further analysis of the tracking system. In the most trivial formulation, a cluster that stems from an electron has also a corresponding electron-track pointing to it. However, as electrons can undergo bremsstrahlung and as photons can convert into electron-positron pairs, deciding whether an electro-magnetic cluster stems from an electron is complex and resource intensive.

The trigger performs a chain of selection criteria on every trigger object hypothesis to discriminate between promising physics within the huge background. This is often called a *trigger chain* (sometimes also called *trigger line* or *trigger path* by different experiments). For every trigger object hypothesis one or more trigger chains are operated in parallel on every event. This includes also combinations of trigger objects, where e.g. two high-$p_{\mathrm{T}}$ muons or jets are asked for.

*2.2.1.* **Exclusive trigger chains** select events according to some well known properties of the wanted physics process, often including event topology and invariant mass cuts, and usually lead to relatively small accept rates. Trigger objects are combined at the trigger level and an event is rejected if none of the wanted topologies is found.

*2.2.2.* **Inclusive trigger chains** try to be as open as possible and select events based on the presence of a single trigger object; e.g. a lepton with a transverse momentum $p_{\mathrm{T}}$ larger than a defined threshold. Inclusive trigger chains can lead to very high accept rates, even beyond the capacity of the data acquisition system for detector read out. A remedy for this is to raise the energy and momentum thresholds for these trigger objects until acceptable rates are obtained that the data acquisition system can handle. Needless to mention that doing so can lead to missing a certain class of physics events.

Therefore, inclusive trigger chains at relatively low energy and momentum thresholds need to be maintained. The high accept rates are reduced based on a random selection; i.e. only every $N^{\mathrm{th}}$ event will be accepted for detector read out, which is often called *pre-scaling*.

*2.2.3.* **Trigger menus** are formed from all trigger chains, exclusive, inclusive, pre-scaled and non-pre-scaled, that are operated together and in parallel during a data taking run.

The trigger menu defines the strategy of selecting events, which are believed in advance of being interesting. I.e. theoretical models and detailed Monte Carlo simulations guide the definition of the trigger menus. Nevertheless, the unexpected shall not be lost and thus trigger menus usually contain a mixture of exclusive and inclusive trigger chains. An example of a trigger menu for the CMS experiment is shown in table 1 below [15, 16]:

An important requirement for every trigger chain in any given trigger menu is its *selection efficiency*, which needs to be as high as possible, bias free and known as precise as possible. Measuring selection efficiencies from data is possible, where a trigger chain is checked offline in a data sample where it was not asked for the primary selection. Potential biases that can be introduced by such methods need to be controlled and cross-checks with pre-scaled trigger chains at reduced transverse energy and momentum thresholds are needed. Often so called minimum bias events are used for the determination of selection efficiencies. Since the probability for finding a high-$p_{\mathrm{T}}$ trigger object in a minimum-bias data sample is usually very low, minimum-bias events are only useful to measure selection efficiencies of trigger chains that themselves require only a moderate-$p_{\mathrm{T}}$. Therefore, low- and/or moderate-$p_{\mathrm{T}}$ trigger objects need to be added to the trigger menu, usually with a high pre-scaling. From there onwards, a recursive procedure can be defined that allows to measure the selection efficiency of all trigger chains.

The trigger menu must also ensure the allocation of adequate bandwidth for calibration, monitoring, and background samples. These must be provided in order

**Table 1.** Example trigger menu for the CMS experiment for a luminosity of $\mathcal{L} = 2 \times 10^{32}\,\mathrm{cm}^{-2}\mathrm{s}^{-1}$. The L1 rates shown are before applying pre-scaling.

| Trigger chain | L1 pre-scale | L1 threshold [GeV] | L1 rate [kHz] | HLT threshold [GeV] | HLT rate [Hz] |
|---|---|---|---|---|---|
| Inclusive electron | 1 | 22 | 4.2 | 29 | 24 |
| Di-electron | 1 | 11 | 1.1 | 12 | 1 |
| Inclusive photon | 1 | 22 | 4.2 | 80 | 3.1 |
| Di-photon | 1 | 11 | 1.1 | 30, 20 | 1.6 |
| Inclusive muon | 1 | 14 | 2.7 | 19 | 26 |
| Di-muon | 1 | 3 | 3.8 | 7 | 4.8 |
| Inclusive tau | 1 | 100 | 1.9 | – | – |
| Di-tau | 1 | 66 | 1.8 | – | 6.0 |
| Single-jet | 1 | 150 | 0.8 | 400 | 4.8 |
| Di-jet | 1 | 100 | 1.7 | 350 | 3.9 |
| Triple-jet | 1 | 70 | 0.7 | 195 | 1.1 |
| Quadruple-jet | 1 | 50 | 0.5 | 80 | 8.9 |
| $b$-jet (leading jet) | 1 | 150, 100, 70, 50 | 1.8 | 350, 150, 55 | 10.3 |
| $H_{\mathrm{T}}^{\mathrm{calo}}$ | 1 | 300 | 1.2 | – | – |
| $E_{\mathrm{T}}^{\mathrm{miss}}$ | 1 | 60 | 0.4 | 91 | 2.5 |
| $H_{\mathrm{T}}^{\mathrm{calo}} + E_{\mathrm{T}}^{\mathrm{miss}}$ | 1 | 200, 40 | 0.7 | 350, 80 | 5.6 |
| tau + $E_{\mathrm{T}}^{\mathrm{miss}}$ | 1 | 100 (tau) | 2.7 | 65 ($E_{\mathrm{T}}^{\mathrm{miss}}$) | 0.5 |
| jet + $E_{\mathrm{T}}^{\mathrm{miss}}$ | 1 | 100, 40 | 0.8 | 180, 80 | 3.2 |
| tau + electron | 1 | 60, 15 | 2.6 | 52, 16 | <1.0 |
| tau + muon | 1 | 40, 7 | 1.2 | 40, 15 | <1.0 |
| Inclusive photon | 400 | 22 | 4.2 | 23 | 0.3 |
| Di-photon | 20 | 11 | 1.1 | 12, 12 | 2.5 |
| Single-jet | 10 | 140 | 1.1 | 250 | 5.2 |
| Single-jet | 1 000 | 60 | 54 | 120 | 1.6 |
| Single-jet | 100 000 | 20 | 1718 | 60 | 0.4 |
| Total rate | | | 23 | | 120 |

to calibrate the detector and to control systematic errors.

Balancing the event rates and the data volume, which can still be handled by the data acquisition system, while maximizing the physics reach of the experiment is just one of those optimizations that will continuously need to be taken care of – throughout the lifetime of an experiment..

Trigger menus especially need to be adjusted following the accelerator instantaneous luminosity, where (some of) the trigger chains need to be pre-scaled or even be disabled completely according the actual instantaneous luminosity, beam and detector conditions and taking into account the priorities of physics goals defined by the collaboration.

## 3. Implementing a trigger and data acquisition system

The trigger has to be capable of implementing the full trigger menu with all trigger chains being executed in parallel. Every trigger chain in turn implies the execution of a

number of sequential steps that step by step validate the trigger chain or reject it. The initial steps need to be executed at the bunch crossing rate dictated by the accelerator, whereas later steps have more relaxed timing constraints.

It is therefore natural to implement a multi-level trigger to execute the sequences of the trigger chains. The first level trigger (L1) has to operate at the collision rate of the accelerator and usually cannot be implemented using commodity components. An implementation based on custom electronics and utilizing fast field programmable gate arrays (FPGAs) and digital signal processors (DSPs) is unavoidable. Only a small subsample of the detector data can realistically be fed into the L1 trigger hardware, and only relatively simple algorithms can be executed. Furthermore, changing algorithms at L1, other than what can be done by re-configuration of pre-scales and threshold values, is close to impossible or implies major upgrades.

For second and third level triggers (L2) and (L3) relaxed requirements on decision latency and data volume exist. This allows the use of more generic processing units and even personal computers (PCs) to be used. The big advantage that follows from such an approach is the utmost flexibility on the trigger algorithms that implement the sequences of every trigger chain. New algorithms accounting for new and better ideas to improve latency, efficiency and robustness for every trigger chain can be added at any time throughout the experiment. Often, triggers implemented based on PC farms are referred to as *high-level triggers* (HLT).

Experiments at Tevatron and LHC have chosen three trigger levels, with the exception of the CMS experiment, which implements just two trigger levels. Table 2 shows the trigger parameters and implementation choices of the CDF, DØ , ATLAS and CMS experiment.

### *3.1. L1 Trigger*

The L1 trigger has to deliver a new decision for every bunch-crossing, which is much shorter time period than the latency it takes for L1 to operate.

A full latency determination starts at the instant the bunches collide, and therefore includes the particle time-of-flight, the cable propagation delay from detector to detector front-end electronics, and the signal propagation time within the front-end electronics. The trigger must wait for the latest detector signal before processing can begin, and in case a positive decision was taken, the LVL1 accept signal needs to travel back to all detector elements to initiate read-out. Considering a typical cable length from a sensitive detector channel to the L1 trigger electronics and back to the detector of $\mathcal{O}(200$ m) and assuming high quality cables capable of transmitting electronic signals at a speed of $\approx 5$ ns/m, latency can not be kept below $\mathcal{O}(\text{few}\,\mu\text{s})$, see also table 2.

*3.1.1.* **Selecting trigger objects at L1 trigger** The L1 trigger accepts candidate trigger objects, which are compatible with the signature of high-$p_{\mathrm{T}}$ leptons, photons and jets, as well as missing energy and total scalar sum of transverse energy. All these

**Table 2.** Trigger parameters at Tevatron and LHC detectors.

| | Tevatron Run II | | LHC | |
|---|---|---|---|---|
| pp centre of mass energy | 1.96 TeV | | 14 TeV | |
| pp inelastic cross section | 50 mb | | 70 mb | |
| Bunch crossing interval | 396 ns | | 25 ns | |
| Bunch crossing rate | 2.5 MHz | | 40 MHz | |
| Peak luminosity | $2-3\times10^{32}$ cm$^{-2}$s$^{-1}$ | | $10^{34}$ cm$^{-2}$s$^{-1}$ | |
| Number of bunches | 36 | | 2808 | |
| Interactions per crossing | $3-4$ | | 25 | |
| Detector | CDF | DØ | ATLAS | CMS |
| Event size | 150 kB | 250 kB | 1.6 MB | 1.0 MB |
| L1 signals | calo/$\mu$/tracking | | calo/$\mu$ | |
| L1 hardware | custom made electronics using ASICs, FPGAs and DSPs | | | |
| L1 rate | 10 kHz | 5 kHz | 100 kHz | 100 kHz |
| L1 latency | 5.5 $\mu$s | 4.2 $\mu$s | 2.5 $\mu$s | 3 $\mu$s |
| L2 signals | L1 information and extra detector information | | Region of Interests | – |
| L2 hardware | custom electronics and generic processors | | 500 PCs | – |
| L2 rate | 350 Hz | 1 kHz | 3.5 kHz | – |
| L2 latency | $\sim$20 $\mu$s | $\sim$100 $\mu$s | $\mathcal{O}(10)$ ms | – |
| L3 signals | full detector read-out fully digitized | | | |
| L3 hardware | 100 PCs | 200 PCs | 1500 PCs | $\sim$2000 PCs |
| L3 rate | 100 Hz | 50 Hz | 200 Hz | 120 Hz |
| L3 latency | $\sim$1 s | $\sim$1 s | $\mathcal{O}(1)$ s | $\mathcal{O}(300)$ ms |

trigger objects deposit energy in the electro-magnetic and hadronic calorimeters, with the exception of muons. It is therefore sufficient to build a L1 trigger decision based on information from the calorimetry and the muon system. However, the rate reduction achievable by L1 based on calorimetric and muon system information alone may not be large enough, and available bandwidth to the L2 trigger system and/or the available computational resources at L2 can become a limiting factor.

The ATLAS and CMS experiments provide enough bandwidth and CPU resources at their next trigger level, whereas the Tevatron experiments DØ and CDF therefore implemented an L1 trigger system that takes tracking into account.

DØ and CDF match muon track segments with tracks found in the inner tracker at L1 to reduced the L1 accept rate further [17, 18].

This is detailed out in the following.

*3.1.2.* **L1 calorimeter trigger** Calorimeters, like e.g. the ATLAS calorimeter have $\mathcal{O}(2\times10^5)$ cells to provide the granularity needed for proper event reconstruction in a high-luminosity environment. Furthermore, raw calorimeter signals extend over many beam crossings, which implies that the information from a sequence of measurements

of signal height in every calorimeter cell needs to be combined in order to estimate the energy deposit and to identify the beam crossing belonging to the energy deposit.

In order to reduce the data volume to be analyzed by the L1 calorimeter trigger, the analog signal of adjacent calorimeter cells are summed to form $\sim$7200 *trigger towers* at a typical granularity of $\Delta\eta \times \Delta\varphi = 0.1 \times 0.1$ in pseudo-rapidity–azimuth space.

The trigger-tower signals are digitized using a dedicated ADC system and digital signal processing is applied to extract the transverse energy $E_{\mathrm{T}}$ for calorimeter pulses and to assign it to the correct bunch crossing, since the shaped pulses from the calorimeters extend over several bunch-crossing periods

A sliding-window algorithm aims to find the optimum region of the calorimeter for inclusion of energy from high-$p_{\mathrm{T}}$ electrons, photons, taus or isolated hadrons by moving a window grid across the calorimeter space so as to maximize the transverse energy seen within the window. A second slightly different sliding window algorithm is performed to find energy deposits originating from high-$p_{\mathrm{T}}$ jets, which uses a coarser granularity of $\Delta\eta \times \Delta\varphi = 0.2 \times 0.2$ in pseudo-rapidity–azimuth space and different configurable window size. The optimum choice will depend on many factors: the jet $E_{\mathrm{T}}$ of interest, the luminosity (level of pile-up within the window), and the need to resolve nearby jets in multi-jet events.

These algorithms are performed in parallel at the beam-crossing rate of 40 MHz and with each trigger tower participation in the calculation of up to 16 windows in both algorithms.

Summation is performed over the trigger towers to calculate the $E_{\mathrm{T}}^{\mathrm{miss}}$ vector and the total scalar $E_{\mathrm{T}}$ for the event. This is done by summing the $E_{\mathrm{T}}$ values over all of the jet elements and the forward calorimeters. In the case of the $E_{\mathrm{T}}^{\mathrm{miss}}$ calculation, the vector energy components are calculated from the $E_{\mathrm{T}}$ values, using lookup tables to multiply by $\sin(\varphi)$ and $\cos(\varphi)$. After summation of $E_x$ and $E_y$ separately, a look-up table is used to compute the scalar $E_{\mathrm{T}}^{\mathrm{miss}}$ value.

The total input bandwidth into the L1 calorimeter trigger system is $\sim$300 GByte/s.

*3.1.3.* **L1 muon trigger** The L1 muon trigger has to identify with high efficiency genuine high-$p_{\mathrm{T}}$ muons, assign them to a particular beam crossing, and determine their transverse momenta and location.

The rate of muons produced in LHC collisions at design luminosity is enormous $\mathcal{O}(1)$ MHz for small muon-$p_{\mathrm{T}}$, as is shown in figure 2.

Muon systems, like e.g. the one for CMS comprise multiple sub-systems with the choice of the detector technologies being driven by the very large surface to be covered and by the different radiation environments.

In the CMS barrel region ($|\eta| < 1.2$), where the neutron induced background is small, the muon rate is low and the residual magnetic field in the chambers is low, drift tube (DT) chambers are used. In the two end-caps, where the muon rate as well as the neutron induced background rate is high, and the magnetic field is also high, cathode strip chambers (CSC) are deployed and cover the region up to $|\eta| < 2.4$. In addition to

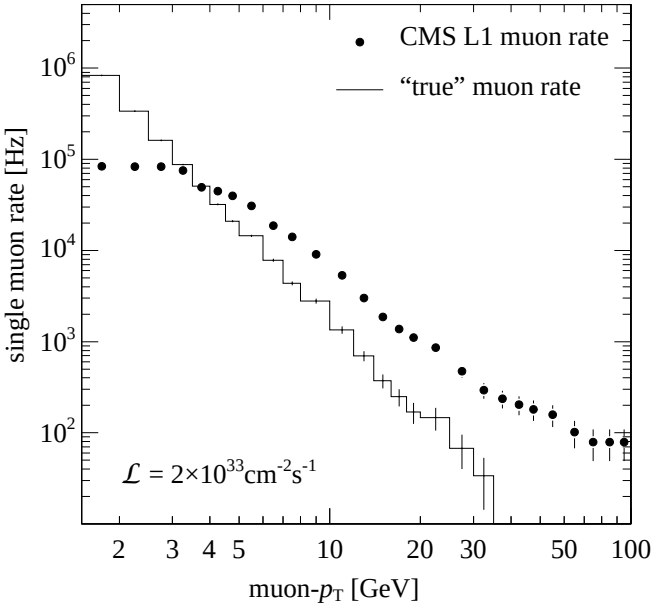


**Figure 2.** CMS L1 trigger rate at $\mathcal{L} = 2 \times 10^{33}\,\text{cm}^{-2}\text{s}^{-1}$ as a function of $p_T$ threshold for single-muons (figure reproduced from [9]).

this, resistive plate chambers (RPC) are used in both the barrel and the end-cap.

The L1 muon trigger of the CMS experiment is based on custom electronics and takes signals from all three muon chamber systems.

The L1 electronics for the DT and CSS chambers first process the information locally, delivering position, direction, bunch crossing, and quality per muon candidate object. Such candidate objects produced by local triggers are often referred to as *trigger primitives*.

The L1 electronics for the RPCs is based on the spatial and time coincidence of hits in four RPC muon stations. The candidate track is formed by a pattern of hits that matches with one of many possible patterns pre-defined for muons with defined transverse momenta. The $p_T$ value is thus given.

Trigger primitives from the DT, CSC and RPC L1 electronics are collected and converted into muon tracks where also transverse momentum $p_T$, pseudo-rapidity $\eta$ and azimuth $\varphi$ are assigned. In addition, the $\eta - \varphi$ coordinates are correlated with the signals from the calorimetric towers to decide whether the muons are isolated.

The CMS L1 trigger electronic is limited to a maximum accept rate of $10^5$ Hz and delivers trigger decisions in 3 $\mu$s at the beam-crossing rate of 40 MHz. Random coincidences, energy-loss fluctuations and multiple-scattering need to be taken into account in the L1 trigger logic and softens the sharpness with which a muon's $p_T$ can be determined. The effect of this can also be seen in figure 2, where the CMS L1 muon rate is shown as a function of the muon-$p_T$. The L1 muon rate is constant just below $10^5$ Hz for muon-$p_T$ $< 3.5$ GeV and falls off softer than the "true" muon rate, which has been generated using Monte-Carlo simulation, for larger values of $p_T$. Even at a $p_T$ threshold of 100 GeV, where signal muon events will be rare, close to 100 Hz of muon

L1 trigger accept rate is expected. A higher level trigger decision is thus needed to re-analyze these muons with greater precision.

*3.1.4.* **L1 tracking trigger** The ATLAS and CMS experiments at the LHC did not chose to build a L1 tracking trigger. However, the CDF and DØ experiments at Tevatron does trigger on tracks already at L1.

The reason for ATLAS and CMS of not implementing tracking triggers at L1 are primarily due to involved complexity and extra costs for with respect to the expected gain in physics coverage. With an L1 accept rate of up to 100 kHz and a data acquisition system providing ample bandwidth to move detector data following a L1 accept to the next trigger level, extra tracking information at L1 becomes redundant. Only in the case where low-$p_{\mathrm{T}}$ physics, where all particles produced in a collision are below threshold of $p_{\mathrm{T}} \approx 3 - 6$ GeV, would need to be studied more carefully, tracking at L1 becomes relevant. The Standard Model use case motivating tracking rigger at L1 is B-physics, where a b-quark fragments into a relatively long-lived B-meson that decays either hadronically or leptonically into particles showing a common displaced vertex with respect to the main $p-p$ collision vertex. Looking again at figure 1, one recognizes a total rate of $b\bar{b}$ production of close to $\sim 10^6$ Hz, which would be unimaginable to handle in a general purpose experiment as ATLAS or CMS. The LHCb experiment is specially built to measure B-physics and its first trigger level has indeed an accept rate of $10^6$ Hz [19]. ATLAS and CMS will play their role in B-physics whenever the B-particle decays in a sufficiently high-$p_{\mathrm{T}}$ muon or muon-pair [20, 21].

At Tevatron the CDF and DØ experiments both implement tracking triggers at L1 [17, 18], which allows them to further reduce the L1 accept rate. Fake muon tracks selected by the L1 muon system, but due to random coincidences, neutron background or from real muons that stem from $K_L^0 \rightarrow \pi\mu\nu_\mu$ decays will thus no-longer contribute to the overall L1 accept rate.

In addition, the CDF experiment also identifies displaced vertices already at L1 which improves the B-physics potential of the CDF experiment.

*3.1.5.* **L1 global trigger** Trigger objects identified by the L1 calorimeter, muon and, if applicable, tracking trigger need to be combined and matched against the trigger menu before a global L1 trigger decision can be taken. This is the task of the *L1 global trigger* (sometimes also called *L1 central trigger* by different experiments). In most experiments this is done by counting the number of isolated and non-isolated L1 trigger objects that are above a predefined set of transverse energy and transverse momentum threshold. In most experiments no exclusive trigger chains can thus be applied in L1 trigger menus.

A special feature worth noting is the capability of the CMS L1 global trigger which also considers topological features of trigger objects based on pseudo-rapidity $\eta$ and azimuth $\varphi$ information [22]. The CMS L1 trigger menu can thus be enriched with a set of exclusive trigger chains. An example being e.g. two isolated electrons or muons

with a back-to-back signature and opposite charge, or any other relative opening angle. Although the ATLAS L1 trigger provides extra geometry information with every L1 trigger object, this information, however available, is not further considered at L1 but directly passed to the L2 trigger.

### *3.2. L2 Trigger*

The strategy of L2 triggers is to refine L1 trigger decisions and to combine trigger objects identified by L1, e.g. in combining data across detectors to form higher quality trigger objects and examining event-wide correlations in all L2 trigger objects.

The DØ and CDF experiments pass the L1 trigger objects and some detector data to the L2 electronics. The L2 triggers for DØ and CDF are both based on a mixture of custom built electronic boards and general purpose processors accepting input signals at the respective L1 accept rates of $\sim 5$ kHz in the case of DØ and $\sim 10$ kHz in the case of CDF. A L2 decision is taken in $\sim 100\mu$s to reduce the event rate further down to $\sim 1$ kHz at DØ and in $\sim 20\mu$s to reduce the event rate further down to $\sim 350$ kHz at CDF.

The differences in the L2 accept rates and latencies for the two experiments is a mere choice of the collaboration. Large latencies imply more time to execute the selection steps for every trigger chain of the trigger menu on the cost of providing larger buffering and also larger processing environment in proportion to the L1 accept rate times latency.

When a large latency of $\mathcal{O}(10)$ ms or higher can be afforded, an interesting possibility opens. It becomes possible to implement the execution of the selection steps in a pure software based environment, providing utmost flexibility in adopting selection strategies and improving trigger menus according the evolving needs and requirements that come up during the whole running time of the experiment.

This has been the choice of the ATLAS and CMS experiment.

The ATLAS L2 trigger is a farm of $\mathcal{O}(500)$ PCs equipped with dual multi-core CPUs. As PCs are commodity devices, they can be easily replaced with faster models and thus a continuous improvement of the total available processing power can be expected.

Every L2 PC in ATLAS treats one or more L1 accepted events in parallel. For every event, information from the L1 trigger is passed to a L2 PC, which consists of so called Region of Interest (RoI) information. The RoI information contains meta data of the L1 trigger objects found, such as trigger object types e.g. electron/photon clusters, jets, $E_{\mathrm{T}}^{\mathrm{miss}}$, muons and their respective trigger thresholds passed, and for every trigger object also their coordinates in pseudo-rapidity $\eta$ and azimuth $\varphi$ space. The L2 PC subsequently collects detector data from the ATLAS read-out system in order to confirm or reject one L1 trigger object after the other, and to refine trigger objects with extra detector data; e.g. in finding tracks from the inner tracker that match with a cluster found in the calorimeter or with a muon track found in the muon system. An

average latency of $\sim 10\,\mu$s of CPU time spent per event is deemed to be sufficient to execute the ATLAS L2 selection. With most events being rejected within $\sim 2-3\,\mu$s, and a correspondingly larger time budget available for more interesting events.

Only about 2% of the data volume of 1.6 MB per event needs to be moved at L1 rate from the detector read-out system to the L2 trigger and analyzed, corresponding to $\mathcal{O}(3)$ GB/s. A dedicated commodity gigabit Ethernet network can handle such data volumes.

An important difference between the ATLAS and the CMS experiment is that the CMS experiment decided against a dedicated L2 trigger as CMS performs the next selection step directly at L3.

### *3.3. L3 trigger*

In all experiments at Tevatron and LHC, the L3 trigger is a computer farm that uses software algorithms for particle identification after event reconstruction. The final rate for writing events to tape is between $50-200$ Hz for the various experiments.

High level triggers (HLTs) are PC farms that are flexible, that do not require special infrastructure for the development of trigger algorithms other than a laptop. In principle complex offline-like algorithms can be executed. On the other side, many hundreds or thousands of PCs need to be operated reliably in a huge farm. Assuring a proper load-balancing when assigning an event to be executed on an individual PC requires non-trivial management of the data flow that also needs to be robust against non-responding PCs due to crashes or other failures.

The CMS experiment decided for a HLT farm capable of absorbing the events at the 100 kHz accept rate of their L1 trigger. The main problem for this is again the data movement, as at a L1 event rate of 100 kHz and a typical event size of 1 MB a total data volume of 100 GB/s arises. The final size of the farm is not yet determined as this depends a lot on the availability of fast multi-core CPUs and the execution speed of the selection software. At an average latency of $\sim 300$ ms per event, one estimates 30 000 CPU cores that need to be operated in parallel [23]. Today, PCs with 8 CPU cores are easily available and PCs with 16 and more CPU cores are expected within a year. This translates to $\mathcal{O}(2000)$ PCs to be operated.

Also ATLAS plans to deploy 2000 PCs for its HLT operation, with $\sim$500 PCs being used for the L2 trigger and $\sim$1500 PCs utilized for the L3 selection.

At the time of this write-up it is not yet clear which of the two approaches will result as the better choice for the experiments trigger selection. As the trigger chains require sequential steps to be executed, the decision taking processes become equivalent in both experiments. The difference however is that in the case of CMS the complete event data is available for processing already after L1, which in principle allows to play sophisticated tricks with some exclusive selection of lower-$p_{\mathrm{T}}$ physics events that otherwise would not have been selected online – assuming availability of enough CPU resources to execute more trigger chains in parallel. Note that also the ATLAS L2 trigger has access to all

detector data - in principle. With more CPU resources available and an upgrade of the commodity gigabit Ethernet network, low-$p_{\mathrm{T}}$ track searches could also be performed in ATLAS.

### *3.4. Triggering the unexpected*

A question that is often asked is whether it is possible to discover physics that was not thought for when defining the trigger chains and when setting up the trigger menu. There is no simple answer to this question. As can be seen from the trigger menu presented in table 1, simple trigger chains have been defined for selecting single-jet events at L1 with a transverse momentum as low as $p_{\mathrm{T}} = 20$ GeV. However, a huge pre-scale value of 100 000 is required to yield an accept rate of 1.7 kHz. If there are enough CPU resources available at the following selection steps, a detailed search for low-$p_{\mathrm{T}}$ phenomena can still be done – with a corresponding loss of available luminosity for such a trigger chain, as given by the pre-scale value.

Another exotic case that can be difficult to trigger on are the production of slow but heavy particles that only decay after having traveled many centimeters or even meters into the detector [24]. As these particles are supposedly slow, they may or may not be associated in the read-out with their original beam-crossing and could appear as a stand-alone events. The original event may or may not show enough missing transverse energy $E_{\mathrm{T}}$ and the decay products of this heavy particle are likely not to match any of the trigger masks that would execute a L1 accept, especially if it decays into muons or even worse, into neutrinos. Thus there is always room for the unexpected to escape detection, even in the most sophisticated trigger systems of today.

## 4. Conclusion and outlook

A powerful and flexible trigger system is decisive in a modern high luminosity collider experiment. It dictates on the physics processes that can be explored and on what is ultimately left unexplored.

Trigger menus need to be carefully composed from trigger chains, which ultimately identify the trigger objects in a sequence of processing steps that define the selection process and span over multiple trigger levels. Discarding unwanted trigger objects early in a sequence of selection steps is key in reducing the overall requirements for bandwidth and CPU resources. The largest fraction of rate reduction is therefore usually performed at the L1 trigger level, which, due to its hardware-based implementation, and fixed wiring, also provides the most rigid infrastructure for event selection.

With the availability of higher bandwidth for read-out and the massive amount of CPU resources that can be provided by means of large CPU farms, the event selection is, wherever possible, no longer performed in a custom built electronics environment, but in a flexible and adaptive software environment, executing selection processing on many hundred or thousands of PCs, all working in parallel.

This trend will continue, as it provides the most flexible environment to adopt new trigger strategies, and to compose new trigger menus containing new ideas for individual trigger chains; e.g. taking into account complex event topologies.

*4.0.1.* **Super LHC** The LHC accelerator is proposed to be upgraded to the Super-LHC (SLHC) [27], where luminosity will be increased by a factor of ten to $\mathcal{L} = 10^{35}$ cm$^{-2}$s$^{-1}$ while the proton-proton centre of mass energy will remain at $\sqrt{s} = 14$ TeV. The beam-crossing interval is likely to double to 50 ns, with its final value not yet concluded. Assuming 50 ns, an average of 500 pile-up events will occur with every beam-crossing, which will lead to higher occupancy and radiation-levels in the detector systems. Replacing some of the detector infrastructure, notably the tracking devices, will likely be required. Regarding the trigger systems, the L1 calorimetric triggers of ATLAS and CMS may just need to be raise their thresholds, whereas the L1 muon triggers will suffer from a higher fake muon rate. This is especially true for the CMS muon system, where multiple scattering of muons in the iron-core has lead to the definition of many more patterns that need to be matched against hits found in the CMS muon systems to form L1 muon tracks. At SLHC, the L1 muon fake rate is likely to be a major issue and a match with L1 tracks from a new to be built inner tracker is being considered [28].

The ATLAS L1 muon system is much less exposed to multiple scattering effects due to its air-core toroid magnet. Therefore, the ATLAS L1 muon trigger is thought to be able to cope even with a ten-fold increase of luminosity.

Average event size will be higher at SLHC, due to higher occupancy in the detector elements. The read-out elements and bandwidth to the PC farms for the higher level triggers, as well as their CPU resources will need to be upgraded. However, the overall strategy, as it has been described in this paper, provides enough flexibility to be also valid at SLHC.

*4.0.2.* **International Linear Collider** The International Linear Collider (ILC) global design [29] effort proposes the next high energy and high luminosity collider to be an electron-positron linear collider at a centre of mass energy of $500 - 1000$ GeV at a luminosity of $\mathcal{L} = 2 \times 10^{34}$ cm$^{-2}$s$^{-1}$. The beam will arrive in a train of 2625 bunches within 970 $\mu$s, with a bunch spacing of 370 ns. Every 200 ms a new train of 2625 bunches will arrive at the collision point, which leaves an interval of 199.3 ms with no collisions. For the trigger and data-acquisition system at a future ILC experiment, an interesting possibility opens. During the 970 $\mu$s, where collisions take place every 370 ns, all the detector signals can be kept in on-detector memories. During the 199.3 ms with no collisions, all the detector signals can be read out and sent to a big PC farm, where the complete trigger menu can be executed. A hardware based L1 trigger, with its rigidity against adopting trigger strategies, is no longer needed; assuming that enough bandwidth for the read-out and enough CPU resources for the execution of the trigger menu can be provided.

As pointed out in section 2, the *ideal* trigger for a high energy and high luminosity collider can become reality at future ILC experiments.

## Acknowledgments

The author likes thank his many colleagues widely spread over many experiments from DØ, CDF, ATLAS and CMS. Without having tea or coffee with many of them at the CERN cafeteria and elsewhere, this article would not have been possible to realize.

## References

[1] DØ Collaboration *The Upgraded DØ Detector* *Nucl. Instrum. Methods* 2006 **A565** 463 http://dx.doi.org/10.1016/j.nima.2006.05.248

[2] CDF Collaboration *The CDF-II Detector: Technical Design Report* Fermilab-PUB-96-390-E (1996) http://www-cdf.fnal.gov/upgrades/tdr/tdr.html

[3] ATLAS Collaboration *Detector and Physics Performance: Technical Design Report, Volume I* CERN/LHCC1999-14 http://cdsweb.cern.ch/record/391176

[4] CMS Collaboration *CMS Physics: Technical Design Report, Volume I, Detector Performance and Software* CERN/LHCC 2006-021 http://cdsweb.cern.ch/record/942733

[5] ALICE Collaboration *ALICE: Physics Performance Report, Volume I* *J. Phys. G: Nucl. Part. Phys.* 2004 **30** 1517–1763 http://dx.doi.org/10.1088/0954-3899/30/11/001

[6] LHCb Collaboration *LHCb: Technical Proposal* CERN/LHCC 1998-004 http://cdsweb.cern.ch/record/622031

[7] TOTEM Collaboration *TOTEM: Technical Design Report, Total Cross Section, Elastic Scattering and Diffraction Dissociation at the Large Hadron Collider at CERN* CERN/LHCC 2004-002 http://cdsweb.cern.ch/record/704349

[8] ATLAS Collaboration *ATLAS High-Level Trigger, Data Acquisition and Controls: Technical Design Report* CERN/LHCC 2003-022 http://cdsweb.cern.ch/record/616089

[9] CMS Collaboration *DAQ generic figures gallery* http://cmsdoc.cern.ch/cms/TDR/DAQ/TDRweb/daqgenericjpg.htm

[10] DØ Collaboration *Search for Neutral Higgs Bosons Decaying to Tau Pairs in $p\bar{p}$ Collisions at $\sqrt{s}$ = 1.96 TeV* *Phys. Rev. Lett.* 2006 **97** 121802 http://dx.doi.org/10.1103/PhysRevLett.97.121802

[11] Djouadi A *Phenomenology of SM and SUSY Higgs bosons at the LHC* Czech. J. Phys. 2005 **55** B23–B44 http://arxiv.org/abs/hep-ph/0412238v1

[12] ATLAS Collaboration $H \to \gamma\gamma$ Chapter 19.2.2 in [25]

[13] The CMS Collaboration *Benchmark channel: $H \to \gamma\gamma$* Chapter 2.1 in [26]

[14] Catani S, Fontannaz M, Guillet J Ph and Pilon E *Cross Section of Isolated Prompt Photons in Hadron-Hadron Collisions* J. High Energy Phys 2002 **0205** 028 http://dx.doi.org/10.1088/1126-6708/2002/05/028

[15] The CMS Collaboration *The Trigger and Data Acquisition project, Volume I+II, Data Acquisition and High-Level Trigger* CERN/LHCC 2000-038 http://cdsweb.cern.ch/record/706847 CERN/LHCC 2002-026 http://cdsweb.cern.ch/record/578006

[16] CMS Trigger, Data Acquisition Group *The CMS High Level Trigger* Eur.Phys.J. **C46** (2006) 605–667 http://dx.doi.org/10.1140/epjc/s2006-02495-8

[17] Holm S et al. *System Architecture and Hardware Design of the CDF XFT Online Track Processor* IEEE Trans. Nucl. Sci. 2000 **47** 895–902 http://dx.doi.org/10.1109/23.856714

[18] Hu Y et al. *The Central Track Trigger of the DØExperiment* IEEE Trans. Nucl. Sci. 2004 **51** 2368–2372 http://dx.doi.org/10.1109/TNS.2004.836090

[19] LHCb Collaboration *LHCb Trigger System Technical Design Report* CERN/LHCC 2003-031 http://cdsweb.cern.ch/record/630828

[20] Panikashvili N for the ATLAS Collaboration *The ATLAS B-Physics Trigger Nucl. Phys.* B (Proc. Suppl.) 2006 **156** 129–134 http://dx.doi.org/10.1016/j.nuclphysbps.2006.03.065

[21] Marinelli N representing the CMS Collaboration *B Physics at LHC with the CMS Detector* AIP Conf.Proc.2004 **722** 225–230 http://dx.doi.org/10.1063/1.1807325

[22] Wulz C E *Concept of the First Level Global Trigger for the CMS experiment at LHC Nucl. Instrum. Methods* 2001 **A473** 231–241 http://dx.doi.org/10.1016/S0168-9002(01)00809-9

[23] Cittolin S *Private communication* 2007

[24] Fairbairn M, Kraan A C, Milstead D A, Sjostrand T, Skands P, Sloan T *Stable massive particles at colliders* Phys. Rept. 2007 **43** 1–63 http://dx.doi.org/10.1016/j.physrep.2006.10.002

[25] ATLAS Collaboration *ATLAS Detector and Physics Performance, Technical Design Report, Volume I+II* CERN/LHCC 1999-014 http://cdsweb.cern.ch/record/391176 CERN/LHCC 1999-015 http://cdsweb.cern.ch/record/391177

[26] The CMS Collaboration *CMS Physics Technical Design Report, Volume I+II, Physics Performance* CERN/LHCC 2006-001 http://cdsweb.cern.ch/record/922757 CERN/LHCC 2006-021 http://cdsweb.cern.ch/record/942733

[27] Azuelos G et al. *Impact of energy and luminosity upgrades at LHC on the physics program of ATLAS J. Phys. G: Nucl. Phys.* **28** 2002 2453–2474 http://dx.doi.org/10.1088/0954-3899/28/9/309

[28] Foudas C, Rose A, Jones J, Hall G *A Study for a tracking trigger at first level for CMS at SLHC* Presented at 11th Workshop on Electronics for LHC and Future Experiments (LECC 2005), Heidelberg, Germany, 12-16 September 2005 http://arxiv.org/abs/physics/0510227

[29] International Linear Collider Global Design Effort *Reference Design Report* http://media.linearcollider.org/rdr_draft_v1.pdf